Polarization resolution of a fiber-based supercontinuum spanning more than 2 octaves

Nicolas Couture[1], Rachel Ostic[1], P. Harshavardhan Reddy[2,3], Ajoy Kumar Kar[4], Mukul Chandra Paul[3], and Jean-Michel Ménard[1]

[1]*Department of Physics, University of Ottawa, Ottawa, ON K1N 6N5, Canada*
[2]*Academy of Scientific and Innovative Research, CSIR-Central Glass and Ceramic Research Institute, Kolkata 700032, India*
[3]*Fiber Optics and Photonics Division, CSIR-Central Glass and Ceramic Research Institute, Kolkata 700032, India*
[4]*Institute of Photonics and Quantum Sciences, Heriot-Watt University, Riccarton Campus, Edinburgh EH14 4AS, UK*

Abstract: We present a novel broadband spectrometer that resolves an orthogonal set of linear polarization states. Our system reveals the frequency-dependent nature of depolarization mechanisms occurring in highly-nonlinear fibers.

OCIS codes: (320.6629) Supercontinuum generation, (060.5295) Photonic crystal fibers, (300.6190) Spectrometers

1. Introduction

Supercontinuum (SC) generation in optical fibers has been rigorously investigated to enable new applications in the fields of optical coherence tomography (OCT), photonic device testing, and optical communication. Silica-based specialty fibers, including GeO_2-doped fibers, are now routinely used to produce these broad and flat optical spectra [1]. Most studies on fiber-based SC sources focus on spectral broadening and flatness but little is known about their polarization properties, which can play a crucial role in three-dimensional OCT imaging [2]. Standard spectroscopic measurement techniques, such as those relying on optical spectrum analyzers (OSAs), offer limited information on the polarization state of the output light associated to each principal axis of the fiber and have hampered experimentalists from exploring depolarization mechanisms over a broadband window. Here, we investigate the SC generated inside a highly GeO_2-doped PCF and its polarization properties as a function of the input polarization state and pulse energy. We use a free-space, broadband, and polarization-sensitive spectrometer allowing us to measure the light in orthogonal polarization states aligned to the principal axes of the highly-nonlinear fiber, revealing frequency-dependent features of depolarization mechanisms.

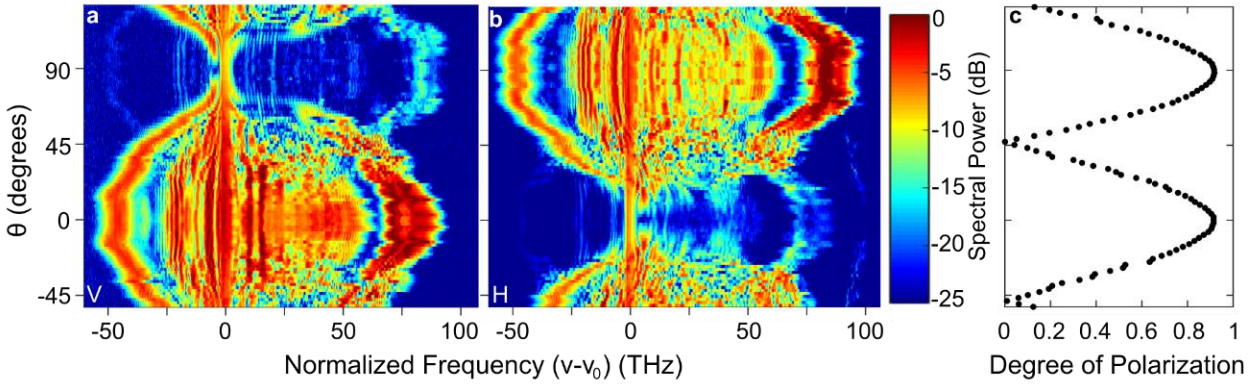

Figure 1. The evolution of the output spectrum of the fiber as the input linear polarization state (θ) is rotated at a fixed input pulse energy of 1.1 nJ and τ = 180 fs. The spectra are centered about the laser frequency $\nu_0 \sim$ 290 THz. We separate the output spectrum into its a) vertical (V) and b) horizontal (H) polarization components. c) The degree of polarization (DOP) of the spectrum calculated from the integrated spectra P_H and P_V, with a maximum value of 0.91 at θ = 0° and 90° - indicating the PCF maintains polarization rather well at this pulse energy and bandwidth.

2. Results and Discussion

Ultrashort pulses centered at 1030 nm, near the zero-dispersion wavelength of the fiber, are injected into a 0.8-meter-long PCF with a coupling efficiency of 40%. The fiber's silica core is characterized by a doping level of 50 mol % of germania with a minimal structural asymmetry and a diameter of 4.7 μm. The input end of the fiber is held fixed while the output end of the PCF is mounted on a rotation stage to align the principal axes of the fiber. These axes are set along the vertical (V) and horizontal (H) directions and an ultrabroadband polarizer is adjusted to isolate the linear polarization state associated to either orientation. The spectra are recorded with a customizable Czerny-Turner configuration monochromator employing three gratings and detectors – allowing for spectroscopic measurements from 400 to 5500 nm. The polarization dependence of the output spectrum of the fiber, centered about the laser

frequency v_0 ~ 290 THz, for an input pulse energy of 1.1 nJ, is shown in Figs. 1a and b. The integrated spectra (P_H and P_V) are used to calculate the degree of polarization, DOP $= |P_V - P_H|/(P_V + P_H)$, and determine the orientation of the principal axes of the PCF (θ = 0° and 90°) at the input. We see that spectral broadening and DOP are maximum when light is injected along one of the principal axes, and minimum when the input polarization is oriented 45° from a principal axis. When injecting a linear polarization state aligned along a principal axis, a fraction of the light is scattered into the orthogonal polarization state due to pressure from the fastening mechanisms holding the fiber ends in their respective v-grooves. This causes the DOP to decrease by ~0.05; imperfections and impurities in the fiber core account for the remaining 0.04 decrease in DOP.

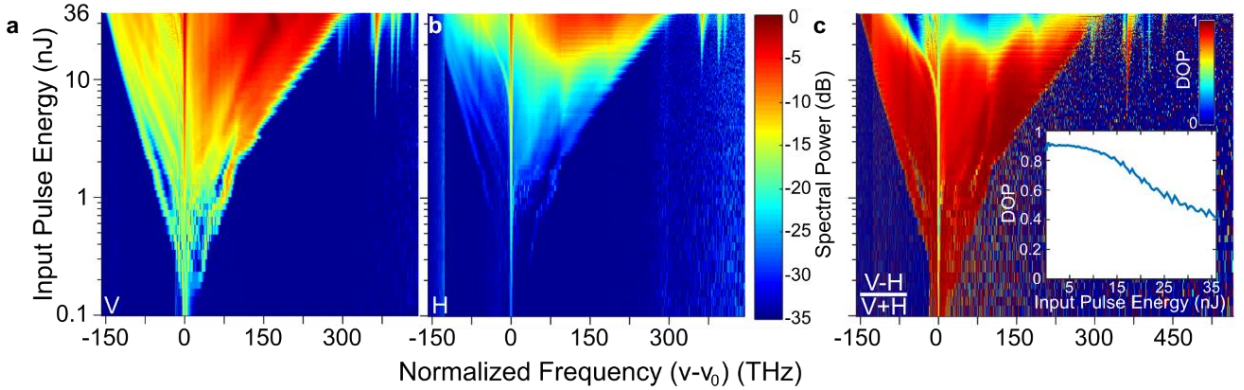

Figure 2. The evolution of the spectrum, separated into its a) V and b) H components, as we increase the pulse energy launched into the fiber from 0.1 nJ to 36 nJ. The spectra are again centered about the laser frequency v_0 ~ 290 THz. The input linear polarization is set along one of the principal axes of the fiber (θ = 0°). c) The DOP of every spectral component using data from a) and b). The inset contains the DOP of the entire spectrum calculated from the integrated spectra in a) and b).

In Figs. 2a and b, we present the evolution of the polarization-resolved output spectrum as a function of input pulse energy. The spectrum is measured for input pulse energies between 0.1 and 36 nJ and θ = 0°. As we increase the pulse energy, we observe the emergence of self-shifted Raman solitons breaking off from the pump towards lower frequencies along with their corresponding dispersive waves extending the SC towards higher frequencies. The broadest spectrum generated spans more than 2 optical octaves. For elevated pulse energies in Fig. 2b, the strong spectral weight in the high-frequency regime indicates a depolarization mechanism favoring higher frequencies. We associate this frequency-dependent depolarization to Rayleigh-scattering in the fiber caused by sub-wavelength defects in the fiber. At the lowest pulse energy in the inset of Fig. 2c, the DOP is 0.91 (consistent with Fig. 1c) and gradually decreases to ~0.4 as the pulse energy is increased. For energies below 5 nJ, the light is mostly contained in V as indicated by the DOP near unity in Fig. 2c and its inset. Plotting the output spectrum of each principal axis as a function of input pulse energy reveals that light scattering into the orthogonal polarization state plays a dominant role in the depolarization process. As light scatters, nonlinear effects in the H polarization result in spectral broadening, decreasing the DOP near the input pump frequency while Rayleigh-like scattering adds to the overall level of depolarization. Conventional techniques would not be able to resolve axis-specific spectra and therefore cannot accurately describe polarization properties of broadband fiber-based spectra.

3. Conclusion

We present a free-space detection scheme that reveals the polarization properties across a broad spectrum generated from a highly-nonlinear GeO_2-doped PCF. The capability of separating the spectrum into orthogonal polarization states aligned to the principal axes of the fiber highlights the role of nonlinear effects and Rayleigh scattering in the depolarization mechanisms. The system we introduce, unlike current methods, allows us to extract the DOP across the entirety of the SC, providing a deeper analysis of the polarization properties of broadband fiber-based sources and therefore establishing itself as the new standard in their characterization. Future work could include the addition of elliptical-sensitive components to this system to fully characterize spectra from twisted fibers designed to guide circularly polarized light.

References

1. D. Jain, R. Sidharthan, P. M. Moselund, S. Yoo, D. Ho, and O. Bang, "Record power, ultra-broadband supercontinuum source based on highly GeO_2 doped silica fiber," Opt. Express **24**, 26667-26677 (2016)
2. J. F. de Boer, C. K. Hitzenberger, and Y. Yasuno, "Polarization sensitive optical coherence tomography – a review [Invited]," Biomed. Opt. Express **8**, 1838-1873 (2017)